

AIRCRAFT CERTIFICATION NOISE LEVELS MINIMIZATION THROUGH THE OPTIMIZATION OF THE TAKEOFF TRAJECTORY

Marcus Vinicius França Barboza, marcus.barboza@embraer.com.br

Pedro Paglione, paglione@ita.br

Instituto Tecnológico de Aeronáutica, Pça. Mal. Eduardo Gomes, 50 – VI. Das Acácias – São José dos Campos – SP - Brasil

Abstract. Noise generated by aircraft during takeoff and approach procedures are today one of the major parameters that will determine if the aircraft will achieve commercial success or even be able to operate in determined airports. One of the most important aircraft noise control tools is on determining the proper takeoff performance, but nevertheless, during conceptual design phase this is still not one of the variables taken into account. When the aircraft is already on an advanced design phase, the potential noise reductions are much smaller and more expensive. The objective of this work is to optimize the thrust cutback procedure in order to minimize the effective perceived noise level (EPNL) on the certification takeoff reference point. The model proposed herein to simulate the aircraft trajectory during takeoff is build from the longitudinal equations of motions and the necessary kinematics relations. Noise is predicted from semi-empirical models, considering the jet and fan noise sources. Sound propagation effects and atmospheric attenuation are also considered.

Keywords: aircraft noise, trajectory optimization, noise certification takeoff performance.

1. INTRODUCTION

A history of individual aircraft noise levels over the last 50 years – see Fig. 1 – shows that there has been a reduction of 20 to 25 dB in the transition from the first turbojet aircraft of the 1950's, through the early turbofans, to the high bypass ratio engines of today. To put this in perspective with the International Civil Aviation Organization (ICAO) most recent recommendation of a 10 dB cumulative reduction (the sum of the reductions at the three certification measurement locations) for new aircraft, this represents a reduction of at least 60 dB. Whichever way the numbers are presented, it has been a major achievement (Sharp, 2004).

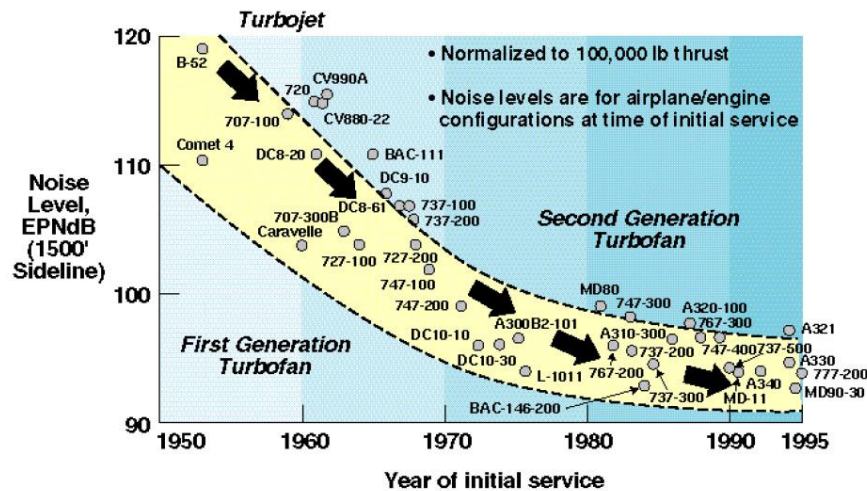


Figure 1. Progress in aircraft noise reduction (Source: Sharp, 2004)

Potential solutions to the problem of airport noise can be divided into the following four elements of a Balanced Approach as defined by ICAO:

- (i) Aircraft noise level reduction
- (ii) Operational procedures
- (iii) Operating restrictions
- (iv) Land-use controls

Due to the current technology in aircraft noise control, further reductions are probably going to be much more difficult, more expensive, and take a long time to achieve. Figure 1 already shows a gradual slowing in the trend of noise reduction with time.

An alternative to reduce the community disturbance due to aircraft noise is to develop special takeoff and landing procedures.

Such procedures, like the noise abatement departure profiles proposed by the USA Federal Aviation Administration (FAA AC 91-53A, 1993) are commonly used and even required by several airports. Several studies have been published to address the airport noise issue by optimizing takeoff and landing. Wijnen and Visser (2003) for example, propose optimal departure trajectories to minimize the sleep disturbance problems in the Amsterdam Schiphol Airport area.

But takeoff profile optimization can be used not only to reduce airport noise but also to reduce the aircraft certificated noise values. The noise certification requirements established by the ICAO and by the FAA, allow the applicant to perform a thrust cutback procedure during takeoff to reduce noise at this noise certification point. The objective of this work is to optimize the two major parameters that define the thrust cutback procedure: when to start the cutback and the percentage of thrust reduction.

2. METHODOLOGY

The simulation tool is composed of a library of routines used to compute many aspects of aircraft performance and noise prediction. Noise modeling is based on semi-empirical methods that account for the engine fan and jet noise sources. Engine performance, as a function of altitude, throttle setting, and Mach number, is estimated using NLR Gas turbine Simulation Program (GSP). The aircraft performance is determined by the solution of the longitudinal equations of motion and the necessary kinematics relations. The optimization tool is the `fmincon` algorithm available in Matlab®.

2.1. Aircraft Performance Model

The longitudinal flight dynamics model is used to simulate the aircraft performance. The model represents the aircraft as a concentrated mass, being the angle of attack the longitudinal control.

Figure 2 shows the reference angles of the longitudinal model. The velocity vector V is tangent to the flight direction. The flight path angle γ is the angle between the horizontal plane and the flight direction given by the vector V . The other angles that define the aircraft longitudinal motion are the pitch angle θ and the angle of attack α .

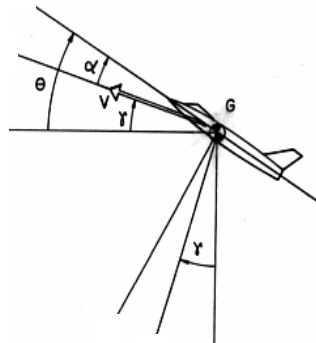


Figure 2. Reference angles of the aircraft longitudinal motion

The external forces are depicted in Fig. 3. Such forces are: lift L , normal to the velocity vector; drag D , parallel but in opposite direction to the velocity; thrust T , with an angle ε with the flight direction and the weight W , parallel to gravity acceleration.

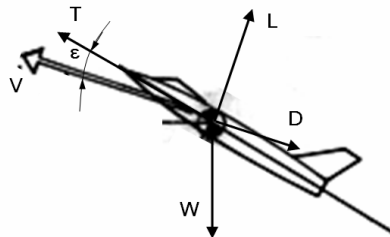


Figure 3. External forces applied in the longitudinal motion

The equations of motion of the longitudinal flight are then

$$T \cos \varepsilon - D - W \operatorname{sen} \gamma = \frac{W}{g} \frac{dV}{dt} \quad (1)$$

$$T \operatorname{sen} \varepsilon + L - W \cos \gamma = \frac{W}{g} V \frac{d\gamma}{dt} \quad (2)$$

In addition to the equations of motion, the following kinematics relations are necessary to determine the vertical (h) and horizontal (x) distances.

$$\dot{x} = V \cos \gamma \quad (3)$$

$$\dot{h} = V \sin \gamma \quad (4)$$

2.1.1. Ground run model

A simplified model is considered for the aircraft ground run. Here, the forces are depicted in Fig. 4, where the aircraft is over a horizontal surface, with the normal reaction R over the landing gears and the horizontal friction component μR .

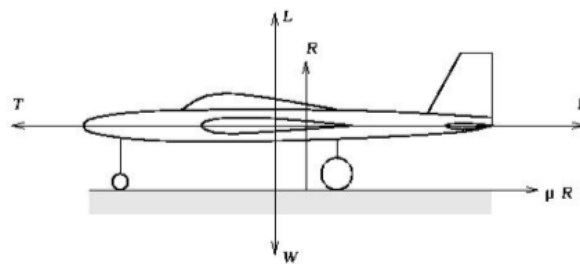


Figure 4. External forces acting over the aircraft during the ground run

The ground run dynamic model is then described by

$$\dot{V} = g \left[\frac{T}{W} - \mu - \frac{1}{W} (D - \mu L) \right] \quad (5)$$

2.2. Aerodynamic Model

The aerodynamic forces acting over the aircraft are described in terms of the non-dimensional lift and drag coefficients C_L and C_D . Where,

$$C_L = \frac{dC_L}{d\alpha} \alpha \quad (6)$$

$$C_D = C_{D0} + k C_L^2 \quad (7)$$

and

$$L = C_L q S \quad (8)$$

$$D = C_D q S \quad (9)$$

where q is the dynamic pressure and S is the wing area. C_{D0} is the friction drag component and k is the lift drag coefficient.

The aerodynamic model also considers the increase in the friction drag component of the total drag due to the deployment of the landing gears and the ground effects in lift and drag that occur when the aircraft is close to the ground surface.

2.2. Engine performance

Developed by NLR, GSP is a component-based modeling environment for gas turbines. Both steady-state and transient simulation of any kind of gas turbine configuration can be performed by establishing a specific arrangement of engine component models.

GSP calculates gas turbine performance, relative to a reference operating point, usually the design point. Off-design steady-state and transient performance is calculated using the customary numerical methods of defining engine system states and solving the equations for the conservation of mass, energy and momentum. (Visser and Broomhead, 2000).

Germane engine performance parameters were determined as a function of altitude, throttle setting, and Mach number using NLR's GSP.

2.3. Noise Estimation

Three measurement points are used by the ICAO and FAA for noise certification. Noise is continuously recorded at these locations during takeoff and landing procedures. Time-integrated sideline, climb, and approach noise (Fig. 5) for a complete takeoff-landing cycle must be below a limit based on the maximum takeoff weight of the airplane (and, for takeoff, the number of engines). Jet noise typically dominates in sideline and climb. On approach, high bypass ratios diminish the contribution of the engine noise at low power, making aerodynamic noise an increasingly relevant component (Antoine and Kroo, 2002).

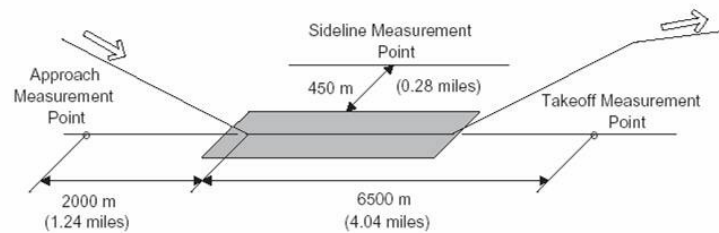


Figure 5. ICAO noise measurement points. (Source: Antoine and Kroo, 2002)

A satisfactory aircraft noise prediction is obtained by a consistent and reliable definition of the aircraft performance; a good prediction of the acoustic characteristics of the engines (as a function of the throttle setting, altitude and flight speed); and for some conditions, the airframe noise (Peart, 1995).

A major source of aircraft noise is the aircraft propulsion system, which main sources are listed below. They are

- (i) jet noise,
- (ii) fan and compressor noise,
- (iii) turbine noise,
- (iv) core noise, which includes combustion noise.

The relative importance of these sources depends largely upon the type of gas turbine and of the flight phase (Fig. 6) (ESDU, 2002).

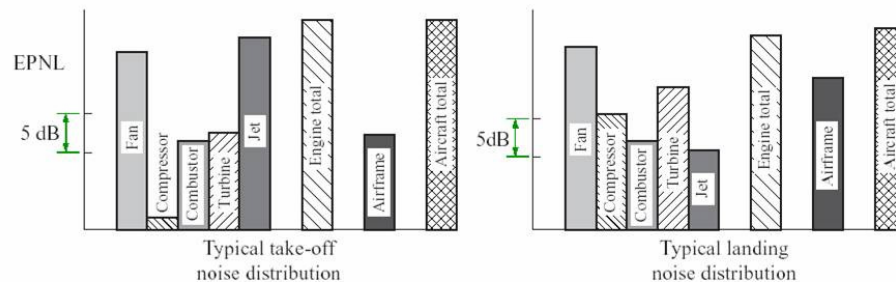


Figure 6. Takeoff and landing noise distributions for a high-bypass ratio turbofan (Source: ESDU, 2002)

The major noise sources for the takeoff of an aircraft equipped with high-bypass ratio turbofan engines are then the fan and jet noise, which are the sources to be modeled herein.

2.3.1. Jet noise

Jet noise is caused by the discharge of the high velocity jet from the engine exhaust (Fig. 7) with potentially three distinct sources: (ESDU, 2002)

- (i) The shearing and turbulent mixing of the exhaust flow with the ambient medium produces jet-mixing noise,
- (ii) Jet shock noise can only occur when the flow is not fully expanded to the local ambient pressure. Shock waves are formed in the flow, which generate noise consisting of both shock-cell screech and shock-associated noise.
- (iii) Finally there is jet entropy noise which only becomes apparent at low velocities and with hot jets.

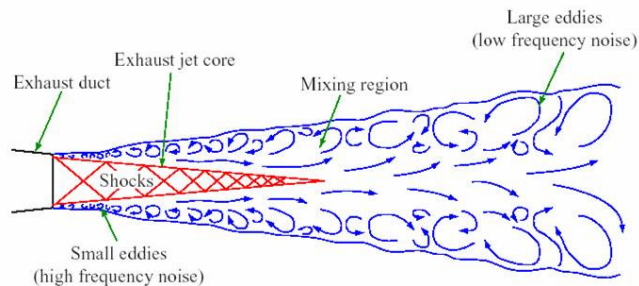


Figure 7. Jet exhaust mixing and shock structure. (Source: ESDU, 2002)

The model used herein to estimate the jet noise is the subsonic coaxial jet mixing noise prediction model compiled by the Society of Automotive Engineers (SAE) (SAE, 1994). This procedure predicts the free-field one-third octave-band sound pressure levels of coaxial subsonic jets for turbofan engines or models under flyover, static and in-flight or in-flow conditions.

The method assumes that the jet mixing process can be subdivided into three noise producing regions, each having its own frequency range. The jet is conceptually divided into three regions; the primary jet, the secondary jet, and the mixed (merged) jet. The three components must, however, to be energy-summed to account for the total jet noise.

2.3.2. Fan noise

An axial-flow fan or compressor produces pressure variations when the rotor and stator blades interact with both smooth and turbulent airflows in the engine. The noise generated falls into three distinct categories:

- (i) blade-passing frequency tones and harmonics,
- (ii) shaft-order tones,
- (iii) broad-band noise.

Items (i) and (ii) are discrete frequency tones produced directly as a result of rotation of the fan or compressor blades. Item (iii) is associated with random phenomena and produces a broad-band spectrum.

There are very few fan noise prediction methods available in the literature, mainly due to sensitive information associated with the development of turbofan engines. The methods available are all variations or improvements of the method proposed by Heidmann (1975).

The method used herein is the Heidmann method with the adjustments proposed by Kontos *et al.* (1996). Kontos *et al.* (1996) identified that the Heidmann method over predicted the tones generated by the fan, and based on several static measurements with the General Electric CF6-80C2, E³ and QCSEE engines proposed some adjustments on the model.

The procedure predicts one-third octave-band levels of the free-field pattern. The noise predictions are applicable to one- and two-stage turbofans with or without inlet guide vanes (IGV). The procedure involves predicting spectrum shape, spectrum level, and free-field directivity for each of the following components:

- (i) fan inlet broad-band noise,
- (ii) fan inlet tone noise,
- (iii) fan inlet combination-tone noise,
- (iv) fan exhaust noise,
- (v) fan exhaust tone noise.

Four parameters are required to predict the basic spectrum levels: mass-flow rate, total temperature rise across the fan stage, and the design and operating point values of the rotor tip relative inlet Mach number. The basic levels are then corrected for presence of IGV, rotor-stator spacing, inlet flow distortions, and cutoff.

2.4. Noise abatement thrust cutback

The thrust cutback procedure is described in the requirements of ICAO and FAA for aircraft noise certification. Figure 8 illustrates a typical takeoff profile. The airplane begins the takeoff roll at point A, lifts off at point B, and begins its first climb at a constant angle at point C. Thrust cutback is started at point D and completed at point E, where the airplane begins a second climb at a constant angle up to point F, the end of the noise certification takeoff flight path. Position K_1 is the takeoff noise measurement station and AK_1 is the distance from start of roll to the flyover measurement point.

Maximum average engine takeoff thrust must be used from the start of takeoff roll to the minimum altitude for initiation of thrust reduction (300 m for two-engine aircraft). The thrust reduction is limited to the greater of:

- (i) that required to maintain one-engine-inoperative level flight, or
- (ii) that required to maintain 4 percent climb gradient with all engines operating.

After thrust reduction a slight decrease in the climb gradient may occur due to the thrust lapse that results from increased altitude during the 10 dB-down period.

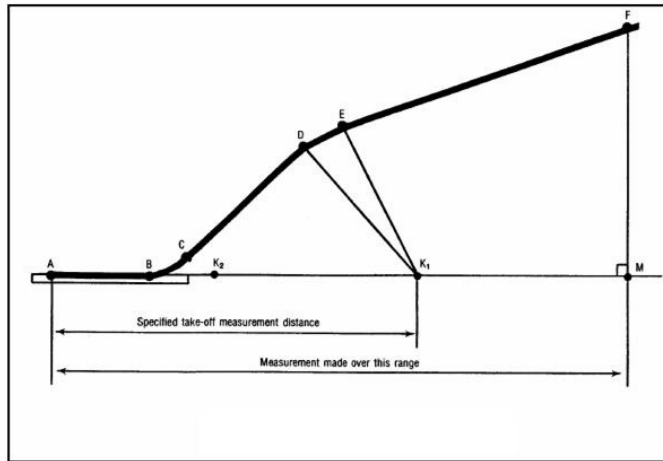


Figure 8. Typical takeoff profile (Source: FAA, 2003)

2.5. Optimization

The optimization framework integrates the all the models described so far for the proper representation of the aircraft takeoff and noise prediction. The longitudinal equations of motions are integrated and the noise level at the takeoff certification point is predicted. The Matlab[®] fmincon algorithm finds, starting on an initial guess, the constrained minimum of the objective function that is the Effective Perceived Noise Level (EPNL) at the flyover noise measurement point.

Two variables are being optimized:

- (i) The altitude above ground level where starts the thrust cutback (subjected to the restriction that it must not be lower than 300 meters for two-engine aircraft), and
- (ii) The percentage of thrust reduction (subject to the restrictions described in Section 2.4).

3. STATEMENT OF THE PROBLEM

As the objective of this work is to minimize the noise level at the flyover noise certification point, the cost function J is the Effective Perceived Noise Level (EPNL). The EPNL is a function of the one-third octave-band spectra for each point of the takeoff trajectory, being then a function of the trajectory history.

The takeoff is performed at a fixed velocity of V_2+10 knots from the 35 ft obstacle, are necessary the solution of only three differential equations to the state determination. These equations are:

$$T \sin \varepsilon + L - W \cos \gamma = \frac{W}{g} V \frac{d\gamma}{dt} \quad (10)$$

$$\dot{x} = V \cos \gamma \quad (11)$$

$$\dot{h} = V \sin \gamma \quad (12)$$

The vector of state has the form

$$\mathbf{y}(t) = \begin{pmatrix} \gamma(t) \\ x(t) \\ h(t) \end{pmatrix} \quad (13)$$

and the control vector $\mathbf{u}(t)$ is

$$\mathbf{u}(t) = \pi(t) \quad (14)$$

Where $\pi(t)$, the thrust control, has the form

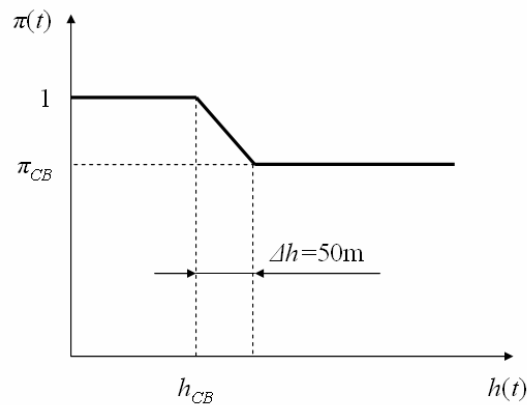


Figure 9. Thrust control function

In fact, the parameters π_{CB} (thrust reduction factor) and h_{CB} (height of start of cutback) are being optimized when optimizing $\mathbf{u}(t)$. The imposed restrictions to the parameters π_{CB} and h_{CB} are the following:

$$\pi_{CB,\min} \leq \pi_{CB} \leq 1.0 \quad (15)$$

$$h_{CB} \geq 300m \quad (16)$$

4. RESULTS

The numerical simulations are based upon the data of a twin-engine airliner developed for educational purposes. Five cases are being analyzed herein:

- (i) takeoff without thrust cutback
- (ii) non-optimized thrust cutback takeoff
- (iii) thrust cutback takeoff with only the thrust cutback reduction factor optimized
- (iv) thrust cutback takeoff with only the thrust cutback initial height optimized
- (v) thrust cutback fully optimized

The noise levels and the control parameters for all cases are presented in Tab. 1.

Table 1. Summary of results

Case	π_{CB} (%)	h_{CB} (m)	EPNL (dB)
i	100.00	$+\infty$	99.93
ii	85.00	300.0	85.02
iii	90.23	300.0	78.12
iv	85.00	500.3	82.35
v	91.55	501.2	76.78

As expected, case (i) resulted in the greater noise levels, since no thrust cutback has been performed in this case. The other four cases are for thrust cutback takeoffs, being case (ii) a non-optimized case. It is clear that the cutback reduces significantly the measured noise, even the non-optimized case resulted in an almost 15 dB reduction.

Cases (iii) and (iv) are to demonstrate which of the two optimizing parameters have the greatest influence in the flyover noise. The optimization of the thrust reduction factor resulted in a reduction of 21.81 dB relative to case (i) and the thrust cutback initial height optimization resulted in a reduction of 17.58 dB. It is clear from these results that the flyover noise is much more sensitive to the thrust reduction factor.

Finally, case (v) is for the optimal combination of the two parameters, with a maximum reduction of 23.15 dB. Figures 10 to 14 show the takeoff trajectories obtained for the five cases.

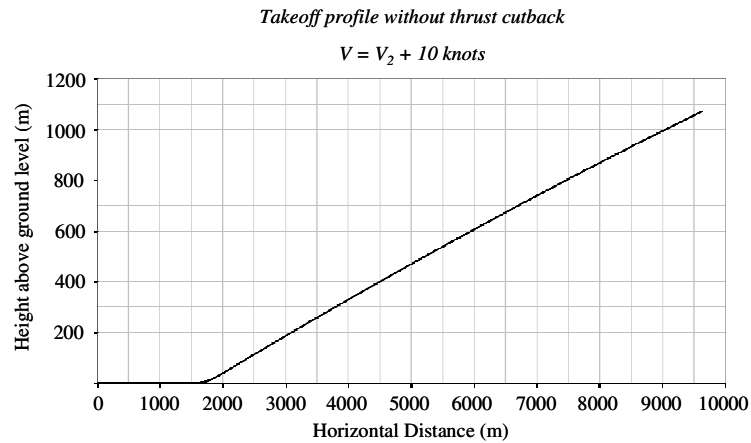


Figure 10. Takeoff profile for case (i)

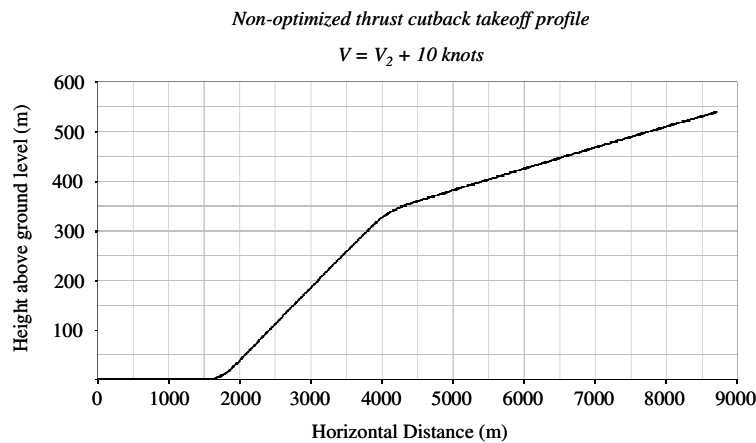


Figure 11. Takeoff profile for case (ii)

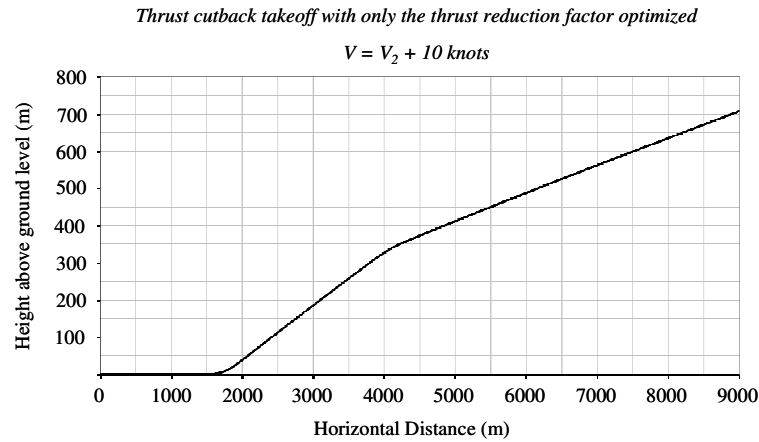


Figure 12. Takeoff profile for case (iii)

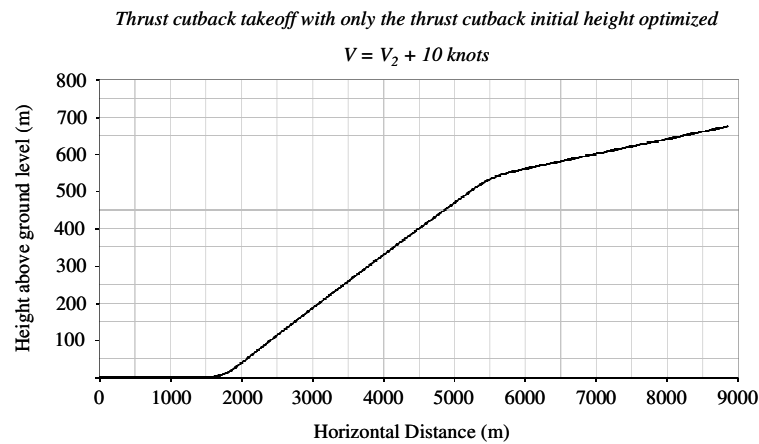


Figure 13. Takeoff profile for case (iv)

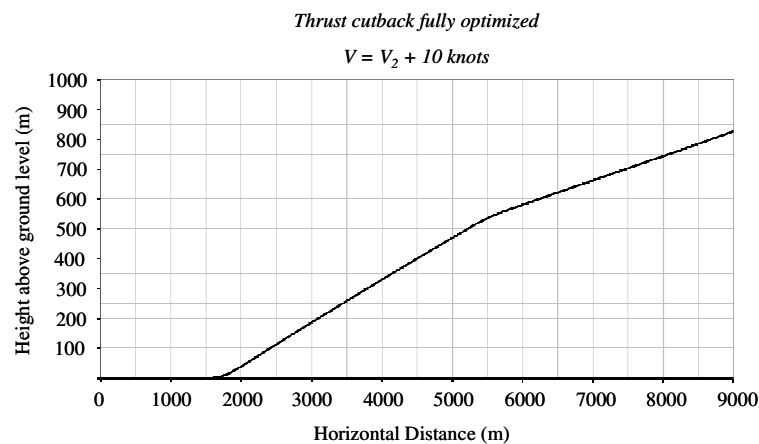


Figure 14. Takeoff profile for case (v)

5. CONCLUSIONS

The objective of this work was to demonstrate that significant certification noise reductions can be achieved by optimizing the noise abatement thrust cutback procedure in the certification takeoff profiles. High fidelity engine and noise models were integrated within an optimization framework producing successful optimal solutions.

It has been shown that the flyover noise level is more affected by the thrust reduction factor than the altitude of the beginning of the procedure, but the optimal combination of the two parameters resulted in the lowest noise.

Upcoming work in refining the noise prediction models and the aircraft performance within this optimization framework can explore other takeoff and landing optimal procedures, achieving further noise reductions without necessarily changing the design of the aircraft.

7. ACKNOWLEDGEMENTS

- Antoine, N.L. and Kroo, I.M., 2002, "Optimizing Aircraft and Operations for Minimum Noise", AIAA's Aircraft Technology, Integration and Operation (ATIO), AIAA 2002-5868, Los Angeles, California, USA
- ESDU, 2002, "ESDU Data Item 02020: An Introduction to Aircraft Noise". ESDU International. London, UK.
- FAA, 1993, Advisory Circular 91-53A: Noise Abatement Departure Profiles. Federal Aviation Administration. Washington, D.C., USA.
- FAA, 2003, Advisory Circular 36-4C: Noise Standards: Aircraft Type and Airworthiness Certification. Federal Aviation Administration. Washington, D.C., USA.
- Heidmann, M.F., 1975, "Interim Prediction Method for Fan and Compressor Source Noise". NASA TM X-71763. National Aeronautics and Space Administration. Washington, D.C., USA.
- Kontos, K.B. Janardan, B.A. and Glibe, P.R., 1996, "Improved NASA-ANOPP Noise Prediction Computer Code for Advanced Subsonic Propulsion Systems. Volume I: ANOPP Evaluation and Fan Noise Model Improvement.". NASA CR-195480. NASA Lewis research Center. Cleveland, Ohio, USA.
- Peart, N.A., 1995, "Flyover-Noise Measurement and Prediction". In: Hubbard, H.H.(ed), Aeroacoustics of Flight Vehicles, Theory and Practice Volume 2: Noise Control, chapter 17. NASA Langley Research Center. Hampton, Virginia, USA.
- SAE, 1994, "Aerospace Recommended Practice 876D: Gas Turbine Jet Exhaust Noise Prediction". Society of Automotive Engineers. Warrendale, Pennsylvania, USA.
- Sharp, B.H., 2004, "Airport Noise Solution for the 21st Century", The 33rd International Congress and Exposition on Noise Control Engineering, 665. Prague, Czech republic.
- Visser, W.P.J. and Broomhead, M.J., 2000, "GSP: A Generic Object-Oriented Gas Turbine Simulation Environment". NLR-TP-2000-267.
- Wijnen, R.A.A. and Visser, H.G., 2003, "Optimal Departure Trajectories with Respect to Sleep Disturbance". Aerospace Science and Technology n.7, pp. 81-91.

8. RESPONSIBILITY NOTICE

The authors are the only responsible for the printed material included in this paper.